A Comparison of Rates of Change in Neuroretinal Rim Area and Retinal Nerve Fiber Layer Thickness in Progressive Glaucoma

Luciana M. Alencar,[1,2] *Linda M. Zangwill,*[1] *Robert N. Weinreb,*[1] *Christopher Bowd,*[1] *Pamela A. Sample,*[1] *Christopher A. Girkin,*[3] *Jeffrey M. Liebmann,*[4] *and Felipe A. Medeiros*[1,2]

Purpose. To evaluate and compare rates of change in neuroretinal rim area (RA) and retinal nerve fiber layer thickness (RNFLT) measurements in glaucoma patients, those with suspected glaucoma, and normal subjects observed over time.

Methods. In this observational cohort study, patients recruited from two longitudinal studies (Diagnostic Innovations in Glaucoma Study–DIGS and African Descent and Evaluation Study-ADAGES) were observed with standard achromatic perimetry (SAP), optic disc stereophotographs, confocal scanning laser ophthalmoscopy (HRT-3; Heidelberg Engineering, Heidelberg, Germany), and scanning laser polarimetry (GDx-VCC; Carl Zeiss Meditec, Inc., Dublin, CA). Glaucoma progression was determined by the Guided Progression Analysis software for standard automated perimetry [SAP] and by masked assessment of serial optic disc stereophotographs by expert graders. Random-coefficients models were used to evaluate rates of change in average RNFLT and global RA measurements and their relationship with glaucoma progression.

Results. At baseline, 194 (31%) eyes were glaucomatous, 347 (55%) had suspected glaucoma, and 88 (14%) were normal. Forty-six (9%) eyes showed progression by SAP and/or stereophotographs, during an average follow-up of 3.3 (±0.7) years. The average rate of decline for RNFLT measurements was significantly higher in the progressing group than in the nonprogressing group (−0.65 vs. −0.11 μm/y, respectively; $P < 0.001$), whereas RA decline was not significantly different between these groups (−0.0058 vs. −0.0073 mm^2/y, respectively; $P = 0.727$). The areas under the receiver operating characteristic (ROC) curves used to discriminate progressing versus nonprogressing eyes were 0.811 and 0.507 for the rates of change in the RNFLT and RA, respectively ($P < 0.001$).

Conclusions. The ability to discriminate eyes with progressing glaucoma by SAP and/or stereophotographs from stable eyes was significantly greater for RNFLT than for RA measurements. (*Invest Ophthalmol Vis Sci.* 2010;51:3531–3539) DOI:10.1167/iovs.09-4350

Glaucoma is by definition a progressive optic neuropathy that advances with characteristic structural damage and corresponding visual field defects. Although most glaucoma patients show some evidence of progression if observed long enough, the rate of structural and functional deterioration can be highly variable among them. In some patients, progression occurs slowly over the course of many years or decades, with minimal impact in the quality of vision. Others, however, have aggressive disease with rapid rates of change that can eventually result in substantial impairment if there are no appropriate medical and/or surgical interventions. Detection of progression and evaluation of rates of change are therefore a fundamental aspect in the management of glaucoma, so that resources can be directed toward the patients who are most likely to have substantial visual impairment by the disease.

Although standard automated achromatic perimetry (SAP) has been the most commonly used method to assess progression, several studies have shown that deterioration of the optic nerve head (ONH) and retinal nerve fiber layer (RNFL) often precede the visual field loss detected by perimetry.[1,2] In fact, changes to the ONH and/or RNFL may be the only signs of progressive disease in many cases. Imaging technologies have added automated analyses to the evaluation of the ONH and RNFL, enabling objective quantification of change in these structures. These technologies have been shown to be useful in the differentiation between glaucomatous and normal eyes, and as predictive tools for future development of visual field loss and optic disc deterioration.[3–10]

One of these imaging technologies, confocal scanning laser ophthalmoscopy (CSLO), has been used to evaluate topographic changes in the ONH, and several studies with CSLO have shown changes in neuroretinal rim area (RA) measurements in glaucoma patients observed over time.[11–18] Another technology, scanning laser polarimetry (SLP), has been developed to evaluate the RNFL, and recent studies have found it promising for detection of glaucomatous change over time.[19–23]

Although investigations have been undertaken to evaluate the ability of these technologies to detect glaucoma progression, no study has yet been performed comparing rates of change in neuroretinal rim and RNFL measurements obtained by these instruments, and there is still a debate as to which one

From the [1]Hamilton Glaucoma Center, Department of Ophthalmology, University of California San Diego, La Jolla, California; the [2]Department of Ophthalmology, University of São Paulo, São Paulo, Brazil; the [3]Department of Ophthalmology, University of Alabama, Birmingham, Alabama; and the [4]Department of Ophthalmology, New York Eye and Ear Infirmary, New York, New York.

Supported by National Institutes of Health Grants EY08208, EY11008, EY14267, EY13959, and EY13959; Pfizer; Eyesight Foundation; and grants for participants' glaucoma medications from Alcon, Allergan, Pfizer, Merck, and Santen.

Submitted for publication July 22, 2009; revised September 12 and November 11, 2009, and January 6, 2010; accepted January 31, 2010.

Disclosure: **L.M. Alencar**, None; **L.M. Zangwill**, Heidelberg Engineering (F), Carl Zeiss (F); **R.N. Weinreb**, Heidelberg Engineering (F), Carl Zeiss (F); **C. Bowd**, None; **P.A. Sample**, Heidelberg Engineering (F), Carl Zeiss (F); **C.A. Girkin**, Heidelberg Engineering (F), Carl Zeiss (F); **J.M. Liebmann**, Heidelberg Engineering (R), Carl Zeiss (R); **F.A. Medeiros**, Heidelberg Engineering (R), Carl Zeiss (F, R)

Corresponding author: Felipe A. Medeiros, Hamilton Glaucoma Center, University of California, San Diego, 9500 Gilman Drive, La Jolla, CA 92093-0946; fmedeiros@eyecenter.ucsd.edu.

of the two structures is more useful as a measure of structural change in glaucoma. The purpose of the present study was to evaluate and compare rates of change in neuroretinal RA and retinal nerve fiber layer thickness in a cohort of glaucoma patients, patients with suspected glaucoma, and healthy individuals observed over time.

METHODS

In this observational cohort study, participants were selected from two ongoing prospective longitudinal studies: the Diagnostic Innovations in Glaucoma Study (DIGS), at the Hamilton Glaucoma Center, University of California, San Diego (UCSD), and the African Descent and Evaluation Study (ADAGES), a multicenter study conducted at the UCSD, the University of Alabama at Birmingham, and the New York Eye and Ear Infirmary. Both studies were designed to prospectively evaluate structural and functional changes in glaucoma, and the same protocols and procedures were used by all three centers. The Reading Centers for both DIGS and ADAGES are housed at the Hamilton Glaucoma Center, University of California, San Diego: The VisFACT (Visual Field Assessment Center) and the IDEA Center (Imaging Data Evaluation and Analysis Center). VisFACT processes and reviews the quality of all visual field test results from standard and function-specific perimetry tests, according to standard protocols. Visual field results are reviewed for the following artifacts: lid and rim, fatigue effects, inappropriate fixation, evidence that the visual field results were due to a disease other than glaucoma (such as homonymous hemianopia), and inattention. The IDEA Center processes and reviews the quality of all simultaneous stereophotographs and also the results from a variety of retinal imaging devices, according to standard protocols. Both centers are responsible for certifying visual field and imaging technicians and photograph graders, processing any data-related queries to the DIGS study coordinator, and requesting that tests be repeated when needed.[24]

All patients from both studies who met the inclusion criteria were enrolled. Informed consent was obtained from all participants, the Human Subjects Committees approved all protocols, and the methods described adhered to the tenets of the Declaration of Helsinki. At each appointment, the subjects underwent a comprehensive ophthalmic examination according to a pre-established protocol, including review of medical history, best corrected visual acuity, slit lamp biomicroscopy, intraocular pressure (IOP) measurement, gonioscopy, dilated funduscopic examination, stereoscopic optic disc photography, and automated perimetry. Only subjects with open angles on gonioscopy were included. Subjects were excluded if they presented best corrected visual acuity $<20/40$, spherical refraction outside ± 5.0 D and/or cylinder correction outside 3.0 D, or any other ocular or systemic disease that could affect the optic nerve or the visual fields.

Patients were tested by SLP (GDx VCC; Carl Zeiss Meditec, Dublin, CA) and CSLO (HRT 3; Heidelberg Engineering, Dossenheim, Germany), as well as standard achromatic perimetry (SAP) and optic disc stereophotographs during the follow-up period. Only good-quality images and reliable visual field results were used. We required a minimum follow-up period of 1 year with each method, a minimum of two visits with the imaging instruments and stereophotographs and a minimum of five visual field tests. As the GDx VCC has been available only since 2002, patients from DIGS and ADAGES who were lost to follow-up before 2002 or who did not have the minimum required number of tests were not be included in the present study. Each patient had exactly the same number of GDx VCC and HRT tests during follow-up. The average number of visits per subject was 4.2 (range, 2–6), with a total of 2565 images provided by each instrument.

The study included patients with diagnosed glaucoma, patients with suspected glaucoma, and healthy subjects. The eyes were classified as glaucomatous based on repeatable abnormal visual field test results at baseline, defined as a pattern standard deviation (PSD) with $P < 0.05$, and/or glaucoma hemifield test (GHT) results outside normal limits, regardless of the appearance of the optic disc. Those with suspected glaucoma had suspicious or glaucomatous appearance of the optic disc (as determined by subjective assessment on the baseline visit) and/or elevated IOP (>21 mm Hg), but normal and reliable SAP visual field results at baseline. Healthy control eyes had no history of elevated IOP, normal appearance of the optic disc, and normal visual fields at baseline. If both eyes of the same patient were eligible for the study, both were included in the analyses. Statistical procedures were used to take into account the correlation between measurements within the same patient. During follow-up, each patient was treated at the discretion of the attending ophthalmologist. Eyes with coexisting retinal disease, uveitis, nonglaucomatous optic neuropathy, or history of intraocular surgery other than for glaucoma or cataract were excluded.

Standard Automated Perimetry

SAP visual fields were tested with either the 24-2 full threshold or Swedish Interactive Thresholding Algorithm (SITA) strategies (Humphrey Field Analyzer, HFA II; Carl Zeiss Meditec, Inc.). Only reliable test results ($\leq$33% fixation losses and false negatives and $<$15% false positives) were included. Glaucomatous progression by visual field was defined by using guided progression analysis (SAP GPA) software version 4.2. Progression by SAP GPA was defined as three or more points, with significant change detected and repeated in three consecutive follow-up tests (probable progression).[25] All cases of progression were evaluated by experts to determine whether the changes detected conformed to glaucomatous progression. To allow progression to be detected by each method during the same period of follow-up, the second baseline for the SAP GPA was matched to the first GDx/HRT image date and the baseline date of the stereophotographs.

Stereophotograph Grading

Simultaneous stereoscopic color optic disc photographs (TRC-SS; Topcon Instrument Corp. of America, Paramus, NJ) were reviewed with a stereoscopic viewer (Pentax Stereo Viewer II; Asahi Optical Co., Tokyo, Japan). For progression assessment, each patient's most recent stereophotograph was compared to the baseline one. Only photographs with adequate quality and clarity were included. The definition of change was based on focal or diffuse thinning of the neuroretinal rim, increased excavation, and detection of new or enlarged RNFL defects. Isolated optic disc hemorrhages and progressive peripapillary atrophy were not considered progression. All graders were masked to identification, temporal sequence of the photographs, and other patient information. Discrepancies between the two graders were resolved by adjudication of a third experienced grader.

Scanning Laser Polarimetry

All patients were imaged with the commercially available scanning laser polarimeter (GDx with Variable Corneal Compensation [VCC], software version 5.0, Carl Zeiss Meditec, Inc.). The general principles of SLP have been published in detail.[26] Only well-focused, evenly illuminated, centered GDx VCC scans with quality score $\geq$7 and typical scan score (TSS) $\geq$80 were included. GDx VCC parameters provided in the standard printout of the instrument and evaluated in this study were superior average, inferior average, and TSNIT average (average of RNFL thickness measurements obtained on a 3.2-mm diameter calculation circle around the optic nerve head: T, temporal; S, superior; N, nasal; and I, inferior). The mean of three images was used for each visit. To evaluate changes in the GDx RNFL measurements in localized sectors and to allow comparison with the sectors evaluated by the HRT, the calculation circle was also divided into six sectors representing the following peripapillary areas: temporal (315–45°), temporal-superior (45–90°), nasal-superior (90–135°), nasal (135–225°), nasal-inferior (225–270°), and temporal-inferior (270–315°), with 0° at the temporal side.

Confocal Scanning Laser Ophthalmoscopy

CSLO images were acquired with the HRT II and analyzed using HRT 3 software (Heidelberg Engineering). Further details on these instru-

ments are provided elsewhere.[27] For each patient, three topographic images were obtained, combined, and automatically aligned to form a single mean topographic image for analysis. Magnification errors were corrected by using the patients' corneal curvature measurements. Good-quality images had to have a focused reflectance image with a standard deviation not greater than 50 μm. The standard reference plane provided by the software was used in all analyses. At the IDEA Center, the optic disc margin was outlined on the mean topography image by trained technicians, while they viewed simultaneous stereoscopic photographs of the optic disc. Topographic parameters included with the HRT software and investigated in this study were global and sectoral RA. The HRT has six sectors: temporal, temporal-superior, temporal-inferior, nasal, nasal-superior, and nasal-inferior. Further, to allow comparison with the sectors provided by the GDx, the two superior and the two inferior HRT sectors were combined into one superior sector and one inferior sector.

Statistical Analysis

Descriptive statistics included the mean and standard deviation for normally distributed variables and median, first quartile, and third quartile values for non-normally distributed variables. Student's *t*-test or Mann-Whitney U test was used to evaluate demographic and clinical differences between progressing, nonprogressing, and healthy subjects.

Progression in this study was defined by visual field results and/or optic disc stereophotograph evaluation during the period of follow-up and was used as the reference to categorize eyes as progressing or nonprogressing. The rates of change (slopes) for RNFL thickness and RA were computed for each subject and compared among groups. Each slope represented the change in RNFL thickness or RA per year, assuming a linear trend across the follow-up period.

Joint linear mixed effects models with random intercepts and random slopes were used to evaluate rates of change in RNFL thickness and RA measurements and their relationship with disease progression, as evaluated by SAP and optic disc stereophotographs. We have used and provided detailed descriptions of the implementation of these models to evaluate change in imaging instruments and longitudinal structure and function associations (Medeiros FA, et al., manuscript submitted, 2009).[19–21] In brief, linear mixed models were used to evaluate the average evolution of each response over time and eye-specific deviations from this average evolution were introduced by random intercepts and random slopes, allowing for different baseline values and different rates of change for each eye. In a joint modeling approach involving mixed models, random effects were assumed for each response process, and the different processes were associated by imposing a joint multivariate distribution on the random effects.

Best linear unbiased predictors (BLUPs) were obtained and used to estimate individual slopes of RNFL thickness and RA change for each eye.[28,29] Receiver operating characteristic (ROC) curves were constructed by using the estimated slopes to evaluate the ability of each parameter to differentiate progressing from nonprogressing eyes. ROC curves show the tradeoff between sensitivity and 1 − specificity. ROC curve areas of 1.0 represent perfect discrimination, whereas areas of 0.5 represent chance discrimination. The areas under the receiver operating characteristic curves (AROCs) for the individual slopes were computed and used to compare the overall accuracy of RNFL thickness and RA for detection of progression. ROC curve areas were compared according to the method of DeLong et al.[30]

To evaluate whether baseline measurements influence the ability to detect loss over time, we also evaluated models including baseline measurements of RNFL thickness and RA (variable *baseline*) and the interaction term with time (*baseline* × *time*) as fixed-effects covariates. As models with and without baseline parameters resulted in similar areas under the ROC curves, we report only the results for the models without the baseline variables.

In statistical analyses, the α level (type I error) was set at 0.05 (STATA ver. 10.0; StataCorp, College Station, TX).

Results

The study included 629 eyes of 390 patients with a mean ± SD age of 55.4 ± 12.0 years. Two hundred fifty (64%) of the patients were women. One hundred seventy-six (45%) of the 390 were of Caucasian ancestry, 209 (54%) were of African ancestry, and 5 (1%) were of Asian descent. At baseline, 194 (31%) eyes were glaucomatous, 347 (55%) had suspected glaucoma, and 88 (14%) were healthy.

Median (first quartile, third quartile) MD and PSD of the visual field closest to the baseline imaging test date in the glaucomatous eyes were −3.27 dB (−4.99, −1.62) and 3.37 dB (2.41, 6.32). Corresponding values for the eyes with suspect glaucoma were −0.22 dB (−1.17, 0.79) and 1.52 dB (1.32, 1.80) and for the healthy subjects, −0.64 dB (−1.51, 0.26) and 1.67 dB (1.41, 1.97). Median (first quartile, third quartile) follow-up was 3.5 years (2.9, 3.9) for the glaucomatous eyes, 3.4 years (2.9, 3.9) for the suspect eyes, and 3.7 years (2.9, 3.9) for the healthy eyes.

From the 541 eyes that were glaucomatous or had suspected glaucoma at baseline, 46 (9%) showed progression over time (26 that had entered the study as glaucomatous eyes and 20 suspect eyes). From the 46 progressing eyes, 26 (57%) progressed only by SAP, 14 (30%) progressed only by optic disc stereophotographs, and 6 (13%) progressed by both methods. Baseline GDx VCC and HRT measurements in progressing, nonprogressing, and healthy control eyes are shown in Table 1. Eyes that showed progression with SAP or stereophotographs had significantly lower RNFL thickness and RA measurements at baseline compared with nonprogressing eyes and eyes of healthy subjects in all parameters, except for temporal RNFL thickness.

Table 2 shows the results of the random-coefficients model regarding changes in average RNFL thickness. The model shows a significant decrease in the measurements over time for both progressing and nonprogressing subjects. However, the rate of decline was significantly higher in the progressing group (−0.65 μm/y) compared with that in the nonprogressing group (−0.11 μm/y). The significance ($P < 0.001$) of the interaction term (*prog* × *time*) indicates that the difference between rates of RNFL loss over time in the two groups was statistically significant. As the nonprogressing group was used as the reference category (0 in the variable *prog*), the coefficient of the variable *time* indicates the rate of loss in the nonprogressing group (as the interaction term *prog* × *time* is 0). The rate of loss in the progressing group is obtained by adding the coefficient for *time* (−0.11 μm/y) to that of the interaction term *prog* × *time* (−0.54 μm/y), which results in −0.65 μm/y. Figure 1 shows a scatterplot of the relationship between baseline measurements of the RNFL thickness and slopes of RNFL loss over time for eyes in which progression was detected by stereophotographs and/or SAP and eyes in which no progression was detected.

Similar models were constructed with measurements for the predetermined sectors. The rates of loss for RNFL thickness for each sector and corresponding *P* values are shown in Table 3 for the comparison of progressing eyes with nonprogressing eyes and in Table 4 for the comparison of progressing eyes with those of healthy subjects. Significant differences in the rate of loss between groups were observed in all sectors. The rates of loss in progressing eyes varied from −0.17 μm/y in the temporal sector to −0.93 μm/y in the nasal-superior sector.

Table 2 also shows the results of the random-coefficients model regarding changes in global RA. The model showed a decrease in the measurements over time in progressing and in nonprogressing eyes. In this case, however, the rates of decline in the progressing (−0.0058 mm^2/y) and the nonprogressing (−0.0073 mm^2/y) groups were not significantly different ($P =$

Table 1. Baseline RNFL Thickness and RA Measurement Summary

	Progressing (n = 46)	Nonprogressing (n = 495)	Controls (n = 88)	P (ANOVA)
RNFL thickness, μm				
Average	46.1 (7.6)	50.1 (7.3)	53.9 (4.6)	<0.001*
Superior	55.5 (11.3)	61.2 (10.4)	66.3 (7.2)	<0.001*
Inferior	51.8 (10.0)	57.2 (10.3)	62.6 (6.0)	<0.001*
Temporal	22.1 (6.8)	21.0 (5.4)	20.7 (4.5)	0.327
Temporal-superior	43.4 (14.1)	48.3 (11.6)	51.6 (9.1)	<0.001*
Temporal-inferior	38.6 (11.6)	44.8 (11.5)	49.9 (8.3)	<0.001*
Nasal	29.8 (5.9)	32.4 (6.8)	34.9 (6.8)	<0.001*
Nasal-superior	46.6 (11.2)	50.5 (11.0)	56.5 (9.6)	<0.001*
Nasal-inferior	51.1 (12.2)	54.8 (10.9)	59.9 (8.2)	<0.001*
RA, mm^2				
Global	1.11 (0.27)	1.33 (0.33)	1.44 (0.27)	<0.001*
Superior	0.15 (0.04)	0.18 (0.05)	0.20 (0.05)	<0.001*
Inferior	0.15 (0.05)	0.19 (0.05)	0.21 (0.04)	<0.001*
Temporal	0.17 (0.07)	0.21 (0.07)	0.23 (0.06)	<0.001*
Temporal-superior	0.14 (0.04)	0.16 (0.05)	0.18 (0.05)	<0.001*
Temporal-inferior	0.13 (0.05)	0.17 (0.06)	0.19 (0.04)	<0.001*
Nasal	0.34 (0.10)	0.39 (0.10)	0.41 (0.09)	<0.001†
Nasal-superior	0.17 (0.05)	0.20 (0.05)	0.21 (0.05)	<0.001
Nasal-inferior	0.17 (0.05)	0.20 (0.06)	0.22 (0.05)	<0.001*
Disc area, mm^2	1.95 (0.50)	2.15 (0.52)	2.07 (0.41)	0.022
Follow-up, y	3.34 (1.00)	3.31 (0.69)	3.39 (0.62)	0.606

* All corresponding pairs (progressing vs. nonprogressing; progressing vs. controls and nonprogressing vs. controls) were significantly different.

† All corresponding pairs except for nonprogressing vs. controls were significantly different.

0.727). Similar models were constructed with RA measurements for the additional predetermined sectors. The rate of loss of RA in each sector and the corresponding P values are shown in Table 3 for the comparison of progressing with nonprogressing eyes and in Table 4 for the comparison of progressing with healthy subjects. No significant differences in the rate of loss between groups were observed in any of the sectors. The rates of loss in progressing eyes varied from -0.0001 mm^2/y in the nasal-inferior sector to -0.0058 mm^2/y for global RA. Figure 2 shows a scatterplot of the relationship between baseline measurements of global RA and slopes showing RA loss over time in eyes that progressed according to stereophotographs and/or SAP and eyes that did not. Since the reference plane is known to vary over time,[31–34] we also created RA models adjusted for reference plane height. Models with reference height produced results similar to the ones without, and therefore we report results only for the latter.

Table 2. Results of the Joint Linear Mixed-Effects Model for Average RNFL Thickness and Global RA, Comparing Progressing and Nonprogressing Eyes

Parameter	Estimate	95% CI	P
Intercept RNFL*	49.97	49.33 to 50.61	<0.001
Prog RNFL†	−3.78	−5.98 to −1.59	0.001
Time RNFL‡	−0.11	−0.18 to −0.04	0.003
Prog × *time* RNFL§	−0.54	−0.78 to −0.30	<0.001
Intercept RA*	1.33	1.31 to 1.36	<0.001
Prog RA†	−0.238	−0.333 to −0.142	<0.001
Time RA‡	−0.0073	−0.0096 to −0.0049	<0.001
Prog × *time* RA§	0.0014	−0.0067 to 0.0096	0.727

* The *intercept* represents the mean value at baseline.

† The significance of the coefficient associated with the variable *prog* indicates whether measurements at a given time are different between progressing and stable eyes.

‡ The significance of the coefficient associated with the variable *time* indicates whether the measurements tend to decrease or increase significantly over time.

§ The two-way interaction *prog* × *time* indicates whether there was a significant difference in change over time between progressing and stable eyes.

Tables 3 and 4 also show the areas under the ROC curves for each parameter for discriminating between progressors and nonprogressors and between progressors and healthy eyes, respectively. The parameter with the best performance to differentiate progressing from nonprogressing eyes was RNFL thickness at the nasal-superior sector (AROC, 0.868; 95% confidence interval [CI], 0.813–0.923). When that sector measurement was compared with average RNFL thickness (AROC, 0.811; 95% CI, 0.741–0.881), the difference was statistically significant (P = 0.035). The highest AROC for RA measurement was for the temporal-inferior sector (AROC, 0.573; 95% CI, 0.475–0.670). However, when that measurement was compared to global RA (AROC, 0.507; 95% CI, 0.404–0.609), the difference was not statistically significant (P = 0.095). The RA slopes neither for HRT sector nor for global RA had ROC curve areas significantly different from 0.5, which represents chance discrimination.

Figure 3 shows ROC curves for average RNFL thickness and global RA. RNFL thickness measurements performed significantly better than did RA measurements ($P < 0.001$) in discriminating progressing from nonprogressing eyes.

Discussion

In this study, we found that higher rates of RNFL loss were significantly related to progression of glaucoma detected by standard methods (i.e., SAP and/or stereophotographs). Progressing eyes had RNFL thickness measurements that decreased at rates several times higher than in nonprogressing eyes during follow-up. In contrast, rates of RA change were not significantly different between progressors and nonprogressors. These findings may have significant implications for the use of these measurements to evaluate and monitor progression in glaucoma patients and patients with suspected glaucoma.

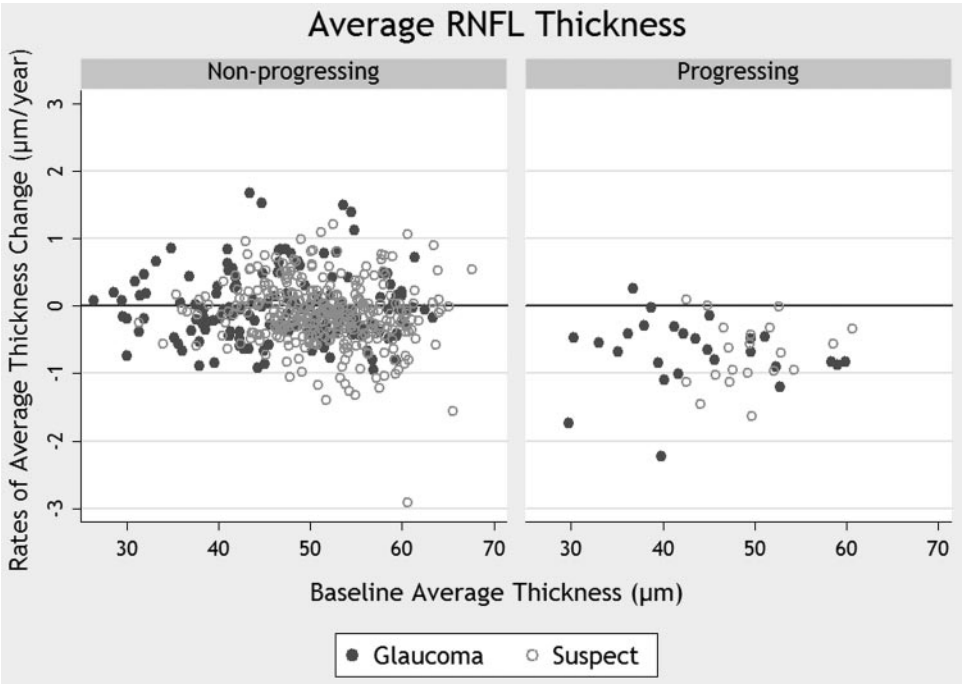

FIGURE 1. The relationship between rates of change in RNFL thickness and baseline measurements. Rates of change are shown for eyes that progressed according to visual field test results and/or stereophotographs (progressing), as well as for eyes that did not (nonprogressing).

Measurements of average RNFL thickness deteriorated at rates on average six times higher in eyes that showed progression by standard methods (−0.65 μm/y) than in those that remained stable (−0.11 μm/y). These results are similar to those in our previous investigation in which we used variable and enhanced corneal compensation algorithms with SLP to evaluate rates of glaucoma progression.[19] Rates of change calculated for the average RNFL thickness performed relatively well in discriminating progressors from nonprogressors, with an area under the ROC curve of 0.811. These findings, now replicated in a larger cohort of subjects, confirm the potential of this technology for longitudinal monitoring of the RNFL in glaucoma. In contrast to the RNFL parameters, rates of RA loss in progressing eyes were similar to those in nonprogressing eyes and the area under the ROC curve for this parameter (0.507) showed a poor discriminatory ability, no better than chance.

It is important to emphasize that estimates of discriminatory capacity as performed in our study depend on the accuracy of visual field test results and stereophotographs when used as reference methods to detect progression. Although widely accepted in clinical practice, the use of SAP and optic disc stereophotographs as reference standards may be subject to criticism. Visual field results and stereophotographs are imperfect reference standards, and it is possible that some of the eyes that were detected as changing by the GDx or HRT but not by

TABLE 3. Average Slopes for Progressing and Nonprogressing Eyes and ROC Curve Areas for the Comparison between the Two Groups

			Rates of Change*		
	AROC	**95% CI**	**Nonprogressing**	**Progressing**	***P***
RNFL thickness					
Average	0.81	0.74–0.88	−0.11	−0.65	<0.001
Superior	0.79	0.72–0.86	−0.21	−0.84	<0.001
Inferior	0.79	0.71–0.86	−0.12	−0.78	<0.001
Temporal	0.70	0.63–0.78	0.09	−0.17	0.036
Temporal-superior	0.72	0.63–0.81	−0.15	−0.65	0.025
Temporal-inferior	0.72	0.64–0.80	−0.21	−0.68	0.032
Nasal	0.78	0.70–0.85	−0.13	−0.49	0.004
Nasal-superior	0.87	0.81–0.92	−0.18	−0.93	<0.001
Nasal-inferior	0.75	0.67–0.83	−0.05	−0.74	0.003
RA					
Global	0.51	0.40–0.61	−0.0073	−0.0058	0.727
Superior	0.55	0.44–0.65	−0.0008	−0.0010	0.773
Inferior	0.52	0.42–0.62	−0.0010	−0.0006	0.590
Temporal	0.45	0.35–0.54	−0.0023	−0.0014	0.541
Temporal-superior	0.55	0.45–0.65	−0.0010	−0.0013	0.729
Temporal-inferior	0.57	0.48–0.67	−0.0012	−0.0011	0.912
Nasal	0.46	0.36–0.55	−0.0012	−0.0008	0.737
Nasal-superior	0.52	0.41–0.62	−0.0006	−0.0007	0.882
Nasal-inferior	0.44	0.33–0.54	−0.0008	−0.0001	0.325

* Slopes given as micrometers/year for RNFL thickness and as millimeters squared/year for RA measurements.

TABLE 4. Average Slopes for Progressing Eyes and Healthy Eyes and ROC Curve Areas for the Comparison between the Two Groups

			Rates of Change*		
	AROC	**95% CI**	**Healthy Subjects**	**Progressing**	***P***
RNFL thickness					
Average	0.82	0.75–0.90	0.01	−0.64	<0.001
Superior	0.78	0.70–0.86	−0.04	−0.85	<0.001
Inferior	0.84	0.77–0.91	0.11	−0.79	<0.001
Temporal	0.79	0.70–0.87	0.12	−0.13	0.072
Temporal-superior	0.74	0.64–0.84	−0.05	−0.65	0.020
Temporal-inferior	0.75	0.67–0.84	0.06	−0.73	0.010
Nasal	0.75	0.66–0.84	−0.17	−0.49	0.025
Nasal-superior	0.83	0.76–0.91	−0.39	−0.95	<0.001
Nasal-inferior	0.89	0.82–0.96	−0.13	−0.76	<0.001
RA					
Global	0.72	0.61–0.83	0.0009	−0.0069	0.141
Superior	0.70	0.60–0.81	0.0003	−0.010	0.049
Inferior	0.69	0.58–0.79	−0.0001	−0.0008	0.387
Temporal	0.77	0.68–0.87	0.0006	−0.0010	0.389
Temporal-superior	0.76	0.67–0.86	0.0004	−0.0013	0.036
Temporal-inferior	0.69	0.59–0.80	−0.0002	−0.0013	0.300
Nasal	0.62	0.51–0.73	−0.0003	−0.0012	0.536
Nasal-superior	0.65	0.53–0.76	0.0001	−0.0008	0.171
Nasal-inferior	0.62	0.51–0.73	0.0001	−0.0002	0.728

* Slopes given as micrometers/year for RNFL thickness and as millimeters squared/year for RA measurements.

conventional methods were in fact true progressors. This discrepancy would underestimate the specificity of the imaging methods in our cohort of subjects. Therefore, we also evaluated rates of change measured by RNFL and RA parameters in completely healthy eyes that had no findings indicative of disease. These rates of change were then compared to those in eyes progressing according to SAP and/or optic disc stereophotographs. In this situation, the area under the ROC curve for rates of change in average RNFL thickness was 0.823, very similar to the area under the ROC curve for discriminating progressors from nonprogressors. For rates of change in RA, although there was an increase in the area under the ROC curve to 0.718, the performance of this parameter can still be considered relatively weak.

It should be noted that the evaluation of the specificity of imaging methods for detection of glaucoma progression using completely healthy eyes is not without problems. In clinical practice, imaging instruments are applied to detect and monitor glaucomatous eyes or eyes with suspected glaucoma. By definition, healthy eyes have different characteristics from the eyes observed in clinical practice, and therefore, estimates of specificity obtained from healthy eyes do not necessarily apply to the clinically relevant population. Also, long-term variability in imaging instruments is likely to be influenced by long-term

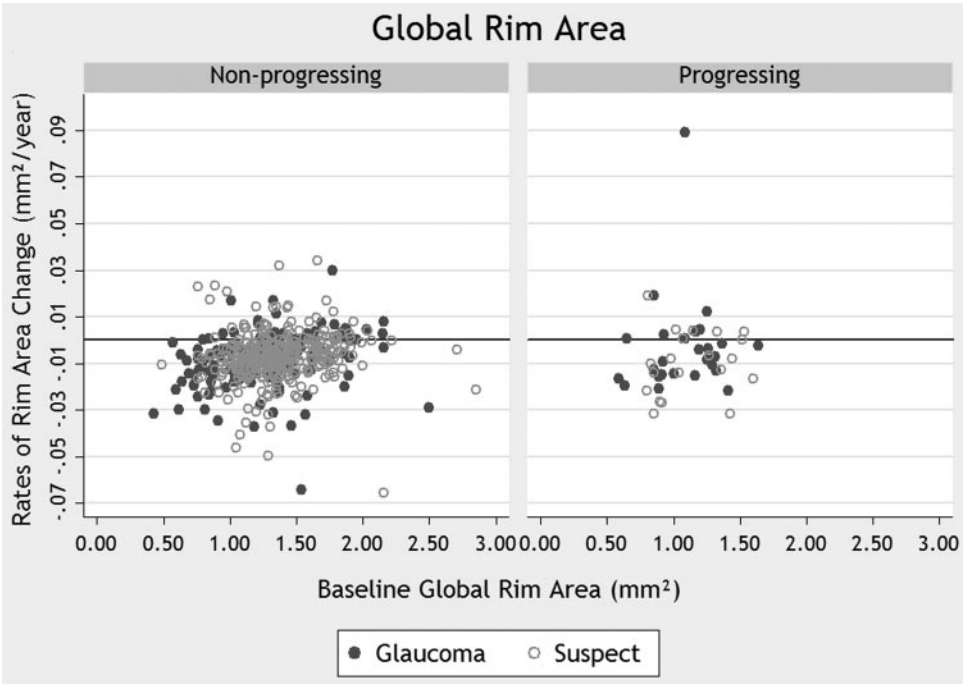

FIGURE 2. The relationship between rates of change in global RA and baseline measurements. Rates of change are shown for eyes that progressed according to visual field test results and/or stereophotographs (progressing), as well as for eyes that did not (nonprogressing).

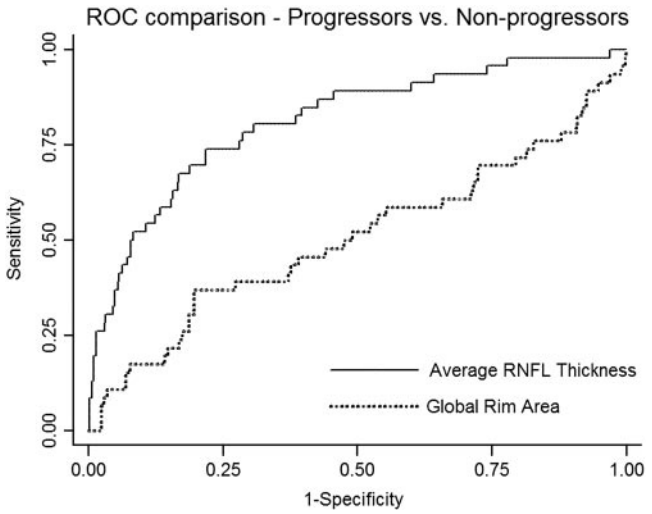

FIGURE 3. ROC curve for average RNFL thickness and global RA.

changes in media opacities or development of other concomitant conditions, which are less likely to occur in completely healthy eyes than in diseased eyes.[21,35]

Several factors have been reported to affect the variability of measurements of neuroretinal RA with CSLO and could be related to the relatively weak performance of these measurements for detecting change over time in our study. One such factor is the fluctuation of IOP. It has been shown that marked reductions of IOP may be associated with relative reversal of the optic nerve head cupping, which may be interpreted as an increase in RA by the instrument.[36–38] In our study, patients were treated at the discretion of the attending ophthalmologist, and it is possible that treatment-related changes in IOP during follow-up affected the ability of CSLO RA measurements to detect change over time. In fact, when we excluded 44 eyes that had undergone glaucoma surgery during follow-up, the rates of neuroretinal loss were significantly different between progressor (-0.020 mm^2/y) and nonprogressor (-0.007 mm^2/y) eyes ($P = 0.015$). In this group, the rates of average RNFL loss were -0.76 μm/y for progressors and -0.13 μm/y for nonprogressors ($P < 0.001$). These findings indicate that CSLO RA measurements seem to be more susceptible to variations in IOP that occur during follow-up of glaucoma patients, which could limit the application of this instrument for monitoring glaucoma progression. Another source of variability is the reference plane height used to calculate RA.[31–34] Rim area measurements are based on an automatically determined standard reference height. Variation on the reference height is associated with variation on RA measurements.[34] New reference planes have been suggested, and future changes in the CSLO software may produce better results for the use of RA in longitudinal analysis of glaucomatous eyes.

The estimated rate of decline in RA found in our study was lower than that reported in a recent longitudinal series of 31 ocular hypertensive subjects in whom repeatable visual field defects developed during the follow-up. Poli et al.[33] reported global RA mean slopes of -0.0123 mm^2/y compared with -0.0058 mm^2/y in our study, with both estimates made using the standard reference plane. Differences in the population between these studies may explain these differences. It has been suggested that structural damage can be better assessed in the early stages of the disease, whereas functional loss may be a better indicator of progression in more advanced stages. We therefore performed a separate analysis including only the 347 eyes with suspected glaucoma (excluding all cases with abnormal visual fields at baseline). The analysis in this group of suspect eyes showed the rate of RA loss in progressing eyes (-0.0145 mm^2/y) to be closer to the one reported in Poli et al.[33] and twice as high as that in stable eyes—however, with no significant statistical difference (-0.0070 mm^2/y, $P = 0.184$).

In our study, the sector with the highest rate of RNFL loss in progressing eyes was the nasal superior, with an average rate of -0.93 μm/y. This location is a relatively unusual one for detection of progressive glaucomatous damage and does not agree with a recent report on the use of SLP to assess progression.[19] We believe this result is related, at least in part, to the more advanced stage of disease in the subjects included in our analysis, as can be observed in comparing the baseline values for RNFL thickness in both studies. In more advanced stages of the disease, the temporal sectors show very thin RNFLs, making it difficult to detect further damage.

The estimates of rates of change obtained in our study were derived from a mixed-effects model and represent best linear unbiased prediction estimates. BLUPs have many advantages over ordinary least squares (OLS) estimates. OLS estimates can be very imprecise in eyes with just a few measurements available over time or with large intraindividual variability.[39] Individual OLS estimates (i.e., individual regression lines) do not take into account the information provided by the whole population. BLUPs are shrinkage estimates that take into account the results obtained by evaluating the whole sample of eyes, giving less weight to estimates obtained in eyes with a small number of measurements and/or large intraindividual variability (that is, more noise).[40] In eyes with a large number of measurements over time, BLUP and OLS estimates give similar results. We have used BLUPs to estimate individual rates of structural change measured by different instruments in glaucoma.[19–21] Others have reported the use of BLUPs to estimate rates of change in longitudinal models of diseases such as Alzheimer's.[41]

The main limitations of our study were the relatively short follow-up time and small number of examinations obtained per patient. These deficiencies could have impaired detection of change in some eyes due to the inherent variability of measurements obtained by imaging devices over time. However, as both methods had exactly the same number of tests during follow-up, we believe that the series length did not significantly affect the comparison between RNFL and RA. We also repeated the analyses including only eyes that had at least five or more tests during follow-up and obtained similar results (data not shown), with significant difference between progressors and nonprogressors for RNFL slopes but not for RA slopes. It should be emphasized, however, that even five images could still be considered a relatively small number and a larger series would result in more precise estimates of rates of change in individual eyes. However, although a large number of tests should be acquired whenever possible, there is a cost associated with obtaining more measurements over time in clinical practice, including the expense of the test itself, the cost in patient time, and the cost related to delaying detection of change. In addition, a linear model with time was used to fit the data. Because of the relatively few measurements available for each test over time, we did not attempt to apply more complicated nonlinear models to the data. Further studies with longer follow-up time and larger image series will be necessary to further evaluate whether other models may provide a better fit to longitudinal measurements from GDx and HRT in glaucoma and the ability of RNFL and RA for detection of glaucomatous progression.

It should also be noted that the RNFL and RA results of this study are specific to the instruments and methods used to obtain the measurements. It is possible that other algorithms for evaluating RA change with the HRT, such as topographic

change analysis (TCA), would perform better in detecting progression with HRT and would more closely represent neuroretinal rim tissue loss, as it does not depend on reference planes. Also, it is possible that the enhanced corneal compensation for SLP would perform better than the GDx VCC for detection of change.

Our study included only GDx VCC and HRT images that were classified as good quality. These images were reviewed by a reading center with certified graders that used standard criteria to evaluate quality. The percentage of images that are classified as poor quality and unusable is also important in the comparison of the utility of these instruments when used for glaucoma monitoring. The average percentage of HRT images that were classified as poor quality by our reading center was 10%, mostly due to SD of the image >50 μm. For the GDx VCC, 5% of the images were classified as poor quality because of an inadequate quality score. An additional 15% of the images were excluded because of the presence of atypical patterns of retardation. It is important to note that refinements in the SLP technology have reduced the prevalence of images with atypical patterns of retardation, which may improve the percentage of usable images with this instrument.

In summary, measurements of rates of change in GDx VCC RNFL thickness were superior to HRT RA in identifying eyes with progression detected by visual field tests or optic disc stereophotographs. Some of the eyes classified as stable by current standard methods may actually have true glaucomatous progression that can be identified by imaging methods; however, further follow-up is necessary to determine the clinical significance of these findings.

References

1. Kass MA, Heuer DK, Higginbotham EJ, et al. The Ocular Hypertension Treatment Study: a randomized trial determines that topical ocular hypotensive medication delays or prevents the onset of primary open-angle glaucoma. *Arch Ophthalmol.* 2002;120(6):701–713; discussion 829–830.
2. Miglior S, Zeyen T, Pfeiffer N, et al. Results of the European Glaucoma Prevention Study. *Ophthalmology.* 2005;112(3):366–375.
3. Mohammadi K, Bowd C, Weinreb RN, et al. Retinal nerve fiber layer thickness measurements with scanning laser polarimetry predict glaucomatous visual field loss. *Am J Ophthalmol.* 2004;138(4):592–601.
4. Medeiros FA, Zangwill LM, Bowd C, Weinreb RN. Comparison of the GDx VCC scanning laser polarimeter, HRT II confocal scanning laser ophthalmoscope, and stratus OCT optical coherence tomograph for the detection of glaucoma. *Arch Ophthalmol.* 2004;122(6):827–837.
5. Deleon-Ortega JE, Arthur SN, McGwin G Jr, et al. Discrimination between glaucomatous and nonglaucomatous eyes using quantitative imaging devices and subjective optic nerve head assessment. *Invest Ophthalmol Vis Sci.* 2006;47(8):3374–3380.
6. Zangwill LM, Bowd C, Berry CC, et al. Discriminating between normal and glaucomatous eyes using the Heidelberg Retina Tomograph, GDx Nerve Fiber Analyzer, and Optical Coherence Tomograph. *Arch Ophthalmol.* 2001;119(7):985–893.
7. Leung CK, Medeiros FA, Zangwill LM, et al. American Chinese glaucoma imaging study: a comparison of the optic disc and retinal nerve fiber layer in detecting glaucomatous damage. *Invest Ophthalmol Vis Sci.* 2007;48(6):2644–2652.
8. Zangwill LM, Weinreb RN, Beiser JA, et al. Baseline topographic optic disc measurements are associated with the development of primary open-angle glaucoma: the Confocal Scanning Laser Ophthalmoscopy Ancillary Study to the Ocular Hypertension Treatment Study. *Arch Ophthalmol.* 2005;123(9):1188–1197.
9. Medeiros FA, Vizzeri G, Zangwill LM, et al. Comparison of retinal nerve fiber layer and optic disc imaging for diagnosing glaucoma in patients suspected of having the disease. *Ophthalmology.* 2008;115(8):1340–1346.
10. Alencar LM, Bowd C, Weinreb RN, et al. Comparison of HRT-3 glaucoma probability score and subjective stereophotograph assessment for prediction of progression in glaucoma. *Invest Ophthalmol Vis Sci.* 2008;49(5):1898–1906.
11. See JL, Nicolela MT, Chauhan BC. Rates of neuroretinal rim and peripapillary atrophy area change: a comparative study of glaucoma patients and normal controls. *Ophthalmology.* 2009;116(5):840–847.
12. Chauhan BC, Nicolela MT, Artes PH. Incidence and rates of visual field progression after longitudinally measured optic disc change in glaucoma. *Ophthalmology.* 2009;116(11):2110–2118.
13. Chauhan BC, Hutchison DM, Artes PH, et al. Optic disc progression in glaucoma: comparison of confocal scanning laser tomography to optic disc photographs in a prospective study. *Invest Ophthalmol Vis Sci.* 2009;50(4):1682–1691.
14. Strouthidis NG, Scott A, Peter NM, Garway-Heath DF. Optic disc and visual field progression in ocular hypertensive subjects: detection rates, specificity, and agreement. *Invest Ophthalmol Vis Sci.* 2006;47(7):2904–2910.
15. Patterson AJ, Garway-Heath DF, Strouthidis NG, Crabb DP. A new statistical approach for quantifying change in series of retinal and optic nerve head topography images. *Invest Ophthalmol Vis Sci.* 2005;46(5):1659–1667.
16. Tan JC, Hitchings RA. Approach for identifying glaucomatous optic nerve progression by scanning laser tomography. *Invest Ophthalmol Vis Sci.* 2003;44(6):2621–2626.
17. Tan JC, Hitchings RA. Optimizing and validating an approach for identifying glaucomatous change in optic nerve topography. *Invest Ophthalmol Vis Sci.* 2004;45(5):1396–1403.
18. Fayers T, Strouthidis NG, Garway-Heath DF. Monitoring glaucomatous progression using a novel Heidelberg Retina Tomograph event analysis. *Ophthalmology.* 2007;114(11):1973–1980.
19. Medeiros FA, Alencar LM, Zangwill LM, et al. Detection of progressive retinal nerve fiber layer loss in glaucoma using scanning laser polarimetry with variable corneal compensation. *Invest Ophthalmol Vis Sci.* 2009;50(4):1675–1681.
20. Medeiros FA, Alencar LM, Zangwill LM, et al. Impact of atypical retardation patterns on detection of glaucoma progression using the GDx with variable corneal compensation. *Am J Ophthalmol.* 2009;148(1):155–163-e1.
21. Medeiros FA, Alencar LM, Zangwill LM, et al. The relationship between intraocular pressure and progressive retinal nerve fiber layer loss in glaucoma. *Ophthalmology.* 2009;116(6):1125–1133-e1–3.
22. Toth M, Hollo G. Increased Long-term measurement variability with scanning laser polarimetry employing enhanced corneal compensation: an early sign of glaucoma progression. *J Glaucoma.* 2008;17(7):571–577.
23. Vermeer KA, Vos FM, Lo B, et al. Modeling of scanning laser polarimetry images of the human retina for progression detection of glaucoma. *IEEE Trans Med Imaging.* 2006;25(5):517–528.
24. Sample P, Girkin CA, Zangwill LM, et al. The African Descent and Glaucoma Evaluation Study (ADAGES): design and baseline data. *Arch Ophthalmol.* 2009;127(9):1136–1145.
25. Leske MC, Heijl A, Hussein M, et al. Factors for glaucoma progression and the effect of treatment: the early manifest glaucoma trial. *Arch Ophthalmol.* 2003;121(1):48–56.
26. Weinreb RN, Shakiba S, Zangwill L. Scanning laser polarimetry to measure the nerve fiber layer of normal and glaucomatous eyes. *Am J Ophthalmol.* 1995;119(5):627–636.
27. Weinreb RN. Laser scanning tomography to diagnose and monitor glaucoma. *Curr Opin Ophthalmol.* 1993;4(2):3–6.
28. Goldberger AS. Best linear unbiased prediction in the generalized linear regression model. *J Am Stat Assoc.* 1962;57(298):369–375.
29. Stanek EJ, 3rd, Well A, Ockene I. Why not routinely use best linear unbiased predictors (BLUPs) as estimates of cholesterol, per cent fat from kcal and physical activity? *Stat Med.* 1999;18(21):2943–2959.
30. DeLong ER, DeLong DM, Clarke-Pearson DL. Comparing the areas under two or more correlated receiver operating characteristic curves: a nonparametric approach. *Biometrics.* 1988;44(3):837–845.

31. Breusegem C, Fieuws S, Stalmans I, Zeyen T. Variability of the standard reference height and its influence on the stereometric parameters of the Heidelberg Retina Tomograph 3. *Invest Ophthalmol Vis Sci.* 2008;49(11):4881–4885.
32. Tan JC, Garway-Heath DF, Fitzke FW, Hitchings RA. Reasons for rim area variability in scanning laser tomography. *Invest Ophthalmol Vis Sci.* 2003;44(3):1126–1131.
33. Poli A, Strouthidis NG, Ho TA, Garway-Heath DF. Analysis of HRT images: comparison of reference planes. *Invest Ophthalmol Vis Sci.* 2008;49(9):3970–3975.
34. Strouthidis NG, White ET, Owen VM, et al. Factors affecting the test-retest variability of Heidelberg retina tomograph and Heidelberg retina tomograph II measurements. *Br J Ophthalmol.* 2005; 89(11):1427–1432.
35. DeLeon Ortega JE, Sakata LM, Kakati B, et al. Effect of glaucomatous damage on repeatability of confocal scanning laser ophthalmoscope, scanning laser polarimetry, and optical coherence tomography. *Invest Ophthalmol Vis Sci.* 2007;48(3):1156–1163.
36. Bowd C, Weinreb RN, Lee B, et al. Optic disk topography after medical treatment to reduce intraocular pressure. *Am J Ophthalmol.* 2000;130(3):280–286.
37. Topouzis F, Peng F, Kotas-Neumann R, et al. Longitudinal changes in optic disc topography of adult patients after trabeculectomy. *Ophthalmology.* 1999;106(6):1147–1151.
38. Lesk MR, Spaeth GL, Azuara-Blanco A, et al. Reversal of optic disc cupping after glaucoma surgery analyzed with a scanning laser tomograph. *Ophthalmology.* 1999;106(5):1013–1018.
39. Beckett LA, Tancredi DJ, Wilson RS. Multivariate longitudinal models for complex change processes. *Stat Med.* 2004;23(2):231–239.
40. Robinson GK. That BLUP is a good thing: the estimation of random effects. *Stat Sci.* 1991;6:15–32.
41. Gould R, Abramson I, Galasko D, Salmon D. Rate of cognitive change in Alzheimer's disease: methodological approaches using random effects models. *J Int Neuropsychol Soc.* 2001;7(7):813–824.